

## RESEARCH ARTICLE

# The formation of microcrystalline defects on the surface of silica glass arising from mechanochemical processing

Boris S. Lunin<sup>1</sup>  | Kirill V. Tokmakov<sup>2,3</sup> 

<sup>1</sup>Department of Chemistry, Lomonosov Moscow State University, Moscow, Russia

<sup>2</sup>College of Engineering and Physical Sciences, Aston University, Birmingham, UK

<sup>3</sup>School of Physics and Astronomy, University of Glasgow, Glasgow, UK

**Correspondence**

Kirill V. Tokmakov, College of Engineering and Physical Sciences, Aston University, B4 7ET, Birmingham, West Midlands, UK.

Email: [k.tokmakov@aston.ac.uk](mailto:k.tokmakov@aston.ac.uk)

**Funding information**

Royal Society Cost Share, Grant/Award Number: IE160125; Russian Foundation for Basic Research, Grant/Award Number: 16-52-10069; Royal Society, Grant/Award Number: IE160125

**Abstract**

The aim of this article is to study the nature of the defects arising on the surface of silica glass during mechanical processing followed by chemical cleaning and etching. Such defects manifest themselves as a narrow Raman peak near  $85\text{ cm}^{-1}$ . It is shown that chemical etching of the ground surface of silica glass leads to the formation of microcrystalline defects embedded at the depth of the near-surface layer. Defects of this kind create heterogeneities in the structure of the atomic network and increase internal friction in silica glass mechanical resonators. This phenomenon should be taken into account when developing the technology for fabrication of high-Q resonators.

**KEYWORDS**

chemical etching, grinding, H8Si8O12, silica glass, surface

## 1 | INTRODUCTION

Mechanical resonators fabricated from pure silica glass show extremely low levels of mechanical loss. The  $Q$ -factor of such resonators (equal to the reciprocal of the loss) exceeds  $10^8$ .<sup>1,2</sup> Low mechanical loss is exploited in hemispherical resonator gyroscopes used for the purpose of navigation.<sup>3–5</sup> Another example of low loss (high- $Q$ ) resonators are the test masses of modern interferometric gravitational-wave detectors.<sup>6–8</sup> The technology for fabricating high- $Q$  resonators includes mechanical grinding (utilized for removing the flaw-rich surface layer) and polishing, followed by (or alternated with) chemical cleaning and etching. Such treatment activates numerous physical-chemical processes on the glass surface. These processes

are stimulated, for example, by the pressure and the high local temperatures that occur at points of contact between grains of the grinding material and the glass surface. The chemical treatment of the silica glass modifies the structure of the surface zone, this can also lead to the appearance of various structural defects. Such alterations of the glass network structure can be detected using Raman spectroscopy. In particular, an intense narrow peak appears in the Raman spectrum near wavenumber  $85\text{ cm}^{-1}$  after mechanical grinding and chemical treatment of a silica glass surface. The peak intensity depends on the surface roughness after grinding and disappears after baking the samples in the flame of an oxy-hydrogen torch. Several types of surface defects have been reported in the literature.<sup>9–11</sup> However, we have not found information

This is an open access article under the terms of the [Creative Commons Attribution](https://creativecommons.org/licenses/by/4.0/) License, which permits use, distribution and reproduction in any medium, provided the original work is properly cited.

© 2022 The Authors. *International Journal of Applied Glass Science* published by American Ceramics Society and Wiley Periodicals LLC.

about any defect linked with an  $85\text{ cm}^{-1}$  spectral peak. In this work, we study the formation and ablation of such defects on the surface of silica glass and compare these processes with experimentally observed changes of mechanical loss (often described in the literature as internal friction).

## 2 | RESEARCH METHOD AND SAMPLES FOR THE EXPERIMENTAL STUDIES

The samples used in these studies were fabricated from the Russian silica glass brands KU-1 (silica glass of type III, using the classification of Bruckner<sup>12</sup>) and KS4V (type IV).<sup>13</sup> Silica glass KU-1 (which is similar to Corning 7940) is produced in the high-temperature pyrolysis reaction of  $\text{SiCl}_4$  in a hydrogen-oxygen flame. The level of impurities in KU-1 is very low, except for the concentration of OH groups, which is 1000–1300 ppm. Silica glass KS4V is similar to Suprasil-311. Details of the manufacturing technology and physical properties have been previously reported.<sup>14</sup> The total content of impurities, including OH groups, is smaller than 1 ppm.<sup>13</sup> For studying surface defects, flat plates  $10\text{ mm} \times 10\text{ mm} \times 1\text{ mm}$  from both brands (KU-1 and KS4V) were used. Some samples were ground with a bonded abrasive tool, where the size of the grit particles was  $50\text{ }\mu\text{m}$ . The roughness of the ground surface was measured to be  $R_a \approx 0.3\text{--}0.4\text{ }\mu\text{m}$ . Other samples of the same size were polished by the supplier of the silica glass; the roughness of these polished samples was as small as  $R_a \approx 0.006\text{ }\mu\text{m}$ . Cylindrical samples with a diameter of 20 mm and a length of 130 mm fabricated from KS4V were ground by a bonded abrasive consisting of grit particles of size 10 and  $28\text{ }\mu\text{m}$ . These samples were used to assess the relationship between the character of surface defects and the level of internal friction.

The samples were chemically etched and cleaned after mechanical processing in such a way that the damaged material was removed from the surface layer by layer. Each cycle of chemical treatment included three steps:

- Etching of the surface layer of the silica glass in an aqueous solution of hydrofluoric acid (HF) with a concentration of 3.6%. A surfactant—perfluoropelargonic acid ( $\text{C}_9\text{HF}_{17}\text{O}_2$ )—was added to the solution. The surfactant concentration in the ready-to-use solution was 0.002%.
- Cleaning in sulfuric acid with a concentration of 40%.
- Cleaning in distilled water.

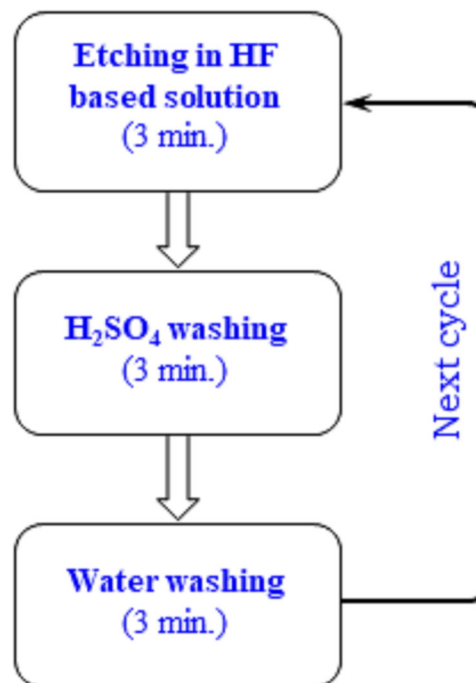


FIGURE 1 A schematic diagram of the chemical treatment. The treatment was conducted at room temperature. The average thickness of the layer removed at each etching cycle was approximately  $0.5\text{ }\mu\text{m}$

The chemical treatment was performed at room temperature and the duration of each stage was 3 min. A schematic diagram of this process is shown in Figure 1.

To control the process of etching, the samples were weighed on a precision balance after three to five consecutive cycles of the chemical treatment. The mass wastage ( $\Delta m$ ) was converted to the thickness of the removed layer ( $h$ ) as follows:

$$h = \frac{\Delta m}{\rho S}, \quad (1)$$

where  $\rho$  is the density of the silica glass and  $S$  is the surface area of the sample.

The Raman spectra were measured using a Fourier spectrometer (EQUINOX 55/S “Bruker”) with excitation wavelength of  $1.064\text{ }\mu\text{m}$ . To facilitate comparison of the results obtained for different samples, the measured scattering intensity was normalized using the intensity of scattered radiation near wavenumber  $\nu \approx 430\text{ cm}^{-1}$ . Figure 2 shows an example of the normalized Raman spectrum for the sample made from KU-1 glass with a ground surface. A narrow peak appears near  $\nu \approx 85\text{ cm}^{-1}$ . Similar spectra with a narrow peak were observed for the ground plates made from the “OH free” glass KS4V. The Raman spectra were measured at a few points on the surface. Each set of

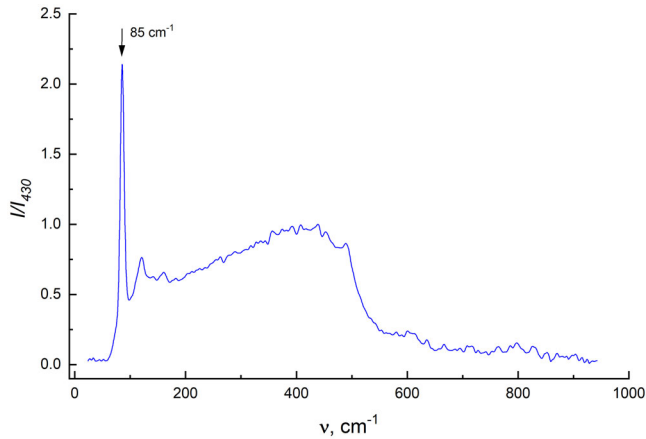


**FIGURE 2** The Raman spectrum for the sample made from glass KU-1 with the ground surface

data was normalized using the intensity of the peak near  $\nu \approx 85/\text{cm}$  ( $I_{85}$ ) and then the results were averaged.

The analysis of the elemental composition of the silica surface was undertaken by means of X-ray photoelectron spectroscopy (XPS) using an Axis Ultra DLD spectrometer (Kratos Analytical). The phase analysis of chemical compounds on the surface of the silica plates was done using an X-ray diffraction technique by means of the diffractometer DRON<sup>15</sup> with Cu K $\alpha$  radiation in the angle range  $3^\circ < 2\theta < 30^\circ$  in increments of  $0.02^\circ$ . The qualitative analysis of the diffractogram was carried out with the software package WinXPow by comparing experimental data with data from the Powder Diffraction File (PDF-2) database.<sup>16</sup> The structure of the surface of the silica plates and the surface roughness were studied using an OLYMPUS LEXT laser microscope and profilometer. We measured surface profiles on several randomly selected sections of the sample surface and calculated the surface roughness. The values obtained were averaged over all areas of the given sample. Silica samples with similar roughness were used for further studies.

To measure internal friction, the cylindrical sample was suspended in a vacuum chamber in equilibrium on a thin tungsten wire (50  $\mu\text{m}$  in diameter). Two pairs of planar electrodes were installed near both faces. One of them (the actuator) was used for the excitation of longitudinal oscillations of the cylinder. To excite mechanical oscillations, we applied an AC voltage of 300–500 V at the resonant frequency  $f$  and a DC offset 500–1000 V to the actuator. The second pair of electrodes was part of the capacitive displacement sensor that transformed the mechanical oscillations into an electrical signal. We characterized the internal friction by the quality factor  $Q$  calculated from the time of free decay  $\tau^*$  of the longitudinal eigenoscillations:

$$Q = \pi f \tau^*. \quad (2)$$

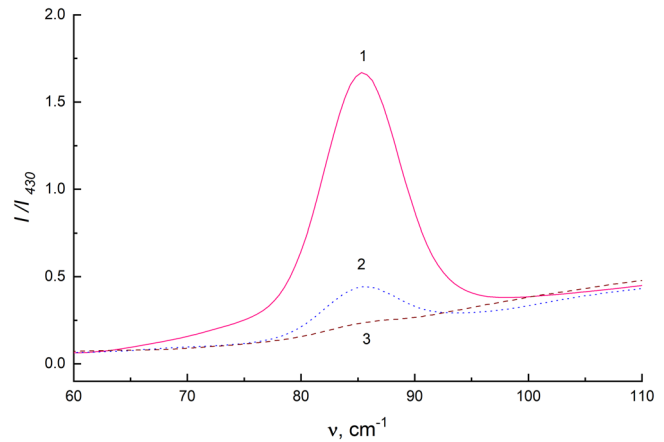


**FIGURE 3** The Raman spectrum for the samples made out of glass KU-1: 1: the sample with the ground surface; 2: the same sample after baking with the flame of a hydrogen-oxygen torch; 3: spectrum measured on a polished sample

The uncertainty provided by this method of measurement was approximately 2%–3%.

The measurement technique is described in greater detail in Lunin and Tokmakov.<sup>2</sup>

### 3 | RESULTS AND DISCUSSION

#### 3.1 | Raman peak $I_{85}$ measured under different surface conditions

The experimental studies have shown that the size of the Raman peak  $I_{85}$  is highly dependent on the quality of the surface treatment. Figure 3 shows the spectrum measured in a narrow frequency band  $\nu \approx 60\text{--}110 \text{ cm}^{-1}$  for samples made from KU-1 silica glass. Curve 1 corresponds to a sample with a ground surface; Curve 2 shows the spectrum of the same sample after baking with the flame of a hydrogen-oxygen torch; Curve 3 represents the spectrum measured on a polished sample.

The spectrum recorded from the ground-surface sample contains an intense peak near wavenumber  $\nu \approx 85 \text{ cm}^{-1}$ . However, its height is sharply reduced after flame treatment. The peak is practically non-existent in the spectrum obtained from the polished sample. The strong dependence of  $I_{85}$  on surface conditions indicates that the defects causing this peak are located in the thin mechanically-damaged surface layer. The structure of this layer is rather complex.<sup>17,18</sup> The outer (most damaged) zone consists of a layer of so-called fissured glass. This zone also contains silica glass microparticles that were split off during mechanical processing. The underlying stratum is a deformed zone containing especially deep cracks while the undamaged material is located beneath. To study the effect of the

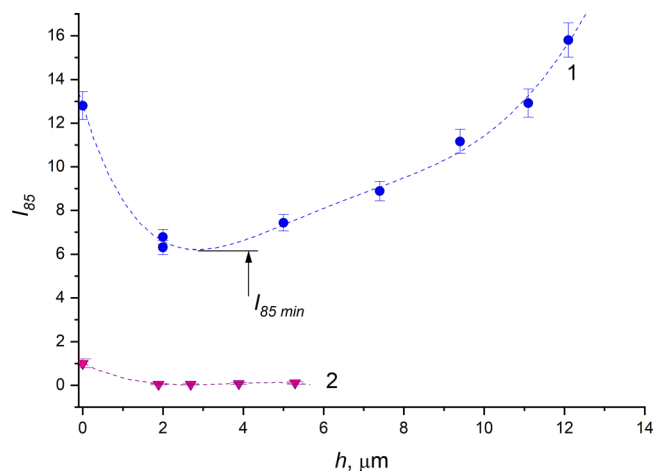


**FIGURE 4** Height of the Raman peak  $I_{85}$  measured on a (1) ground and (2) polished silica glass sample plotted against the thickness of the removed surface layer

surface layer zones on the height of the  $I_{85}$  peak, we etched both ground and polished samples. Typical results are shown in Figure 4.

As seen in the figure,  $I_{85}$  in the Raman spectra of a ground surface decreases rapidly when removing a layer of thickness 2–5  $\mu\text{m}$ , reaching a minimum of  $I_{85\text{min}} \approx 6$  relative units. Further chemical etching of the sample with a ground surface leads to a monotonic increase of  $I_{85}$ . After removing 12  $\mu\text{m}$  of the surface layer, the height of the peak  $I_{85}$  even exceeds the initial level. The value of  $I_{85}$  observed on polished samples is much smaller. After removal of a thin layer at the very first stage of etching,  $I_{85}$  has become close to zero and is not changed by further processing.

The initial decrease of the peak  $I_{85}$  can be linked to the removal of the outer surface layer. The glass shards (the silica micro-particles) being removed at this stage from the ground surface contain a large number of structural defects. The rougher surface contains more such shards cleaved off during the grinding process. This would explain the big difference in  $I_{85}$  for surfaces of different roughness.

The subsequent rise of  $I_{85}$  after further chemical treatment suggests that the defects grow again, likely from seeds created by mechanical treatment. Such seeds are located below the removed surface layer (2–5  $\mu\text{m}$ ), possibly close to the bottom of large surface cracks. The depth of surface cracks corresponding to the measured roughness of the ground samples can be as large as 18–20  $\mu\text{m}$ .<sup>19</sup> Obviously, the polished surface contains no such defects. That is why  $I_{85}$  does not change during etching of the polished surface but rises substantially during etching of the ground surface.

To identify specific defects causing the  $I_{85}$  peak in the Raman spectrum, we studied the surface using a laser microscope and profilometer. Figure 5 shows a micrograph

of a silica glass plate after removing  $\sim 15 \mu\text{m}$  of the surface layer. The inclusions that arose after the chemical treatment are distinctive due to their different color and structure.

An additional study was undertaken with the XPS spectrometer. Obviously, peaks corresponding to oxygen and silicon clearly dominated the XPS spectrum. One would also expect the appearance of any products of chemical reactions between  $\text{SiO}_2$  and HF or  $\text{H}_2\text{SO}_4$  used in the etching and cleaning procedure. However, we did not observe peaks corresponding to fluorine and sulfur.

An X-ray phase analysis of the glass samples also was carried out. Figure 6 presents a diffractogram of the ground plate made from KU-1 glass. The reflexes (the peaks) clearly visible on the diffractogram correspond to angles  $2\theta = 12.4^\circ$  and  $2\theta = 24.9^\circ$ .

We compared the parameters of these reflexes with the PDF-2 database<sup>16</sup>; in our view, the crystalline defects formed on the surface of the silica glass samples may plausibly be identified as octahydrodoctasilsesquioxane ( $\text{H}_8\text{Si}_8\text{O}_{12}$ ).

This conclusion is consistent with the results obtained by Raman spectroscopy. According to previous studies,<sup>20–22</sup> the Raman spectrum of  $\text{H}_8\text{Si}_8\text{O}_{12}$  contains a peak at  $\nu \approx 84 \text{ cm}^{-1}$ . The binding of  $\text{H}_8\text{Si}_8\text{O}_{12}$  cluster molecules to dangle SiO bonds has also been reported in the literature.<sup>23</sup>

It should be noted that the height of the  $84 \text{ cm}^{-1}$  peak observed in the previous studies<sup>21,22</sup> was smaller than the heights of the other peaks in the Raman spectrum. However, Bärtsch et al.<sup>21</sup> and Bornhauser and Calzaferri<sup>22</sup> studied crystalline powdered  $\text{H}_8\text{Si}_8\text{O}_{12}$ . The technology used for the fabrication of the powder, the surface conditions, and the size of the particles were not reported. We can assume that the heights of the peaks may depend on the size of the crystals, as well as on the concentration of dislocations in surface microcrystals or powder grains. The crystalline defects reported in our article were formed in very specific conditions: their size and the distribution of dislocations are almost certainly different. Supposedly, these two factors may affect the Raman spectra. That is why the discrepancy between our results and the spectra reported in previous studies<sup>21,22</sup> is not necessarily contradictory. Certainly, though, the  $\text{H}_8\text{Si}_8\text{O}_{12}$  hypothesis requires further consideration.

Octahydrodoctasilsesquioxane ( $\text{H}_8\text{Si}_8\text{O}_{12}$ ) has a crystalline structure<sup>24</sup>; the cluster visualization is shown in Figure 7. The data obtained here do not allow a clear explanation of the formation of  $\text{H}_8\text{Si}_8\text{O}_{12}$  under these conditions. We think these defects are formed during the wet grinding and chemical processing of the surface in aqueous solutions, when the intermolecular bonds cleaved by cracks are being hydroxylated, that is, while the OH groups



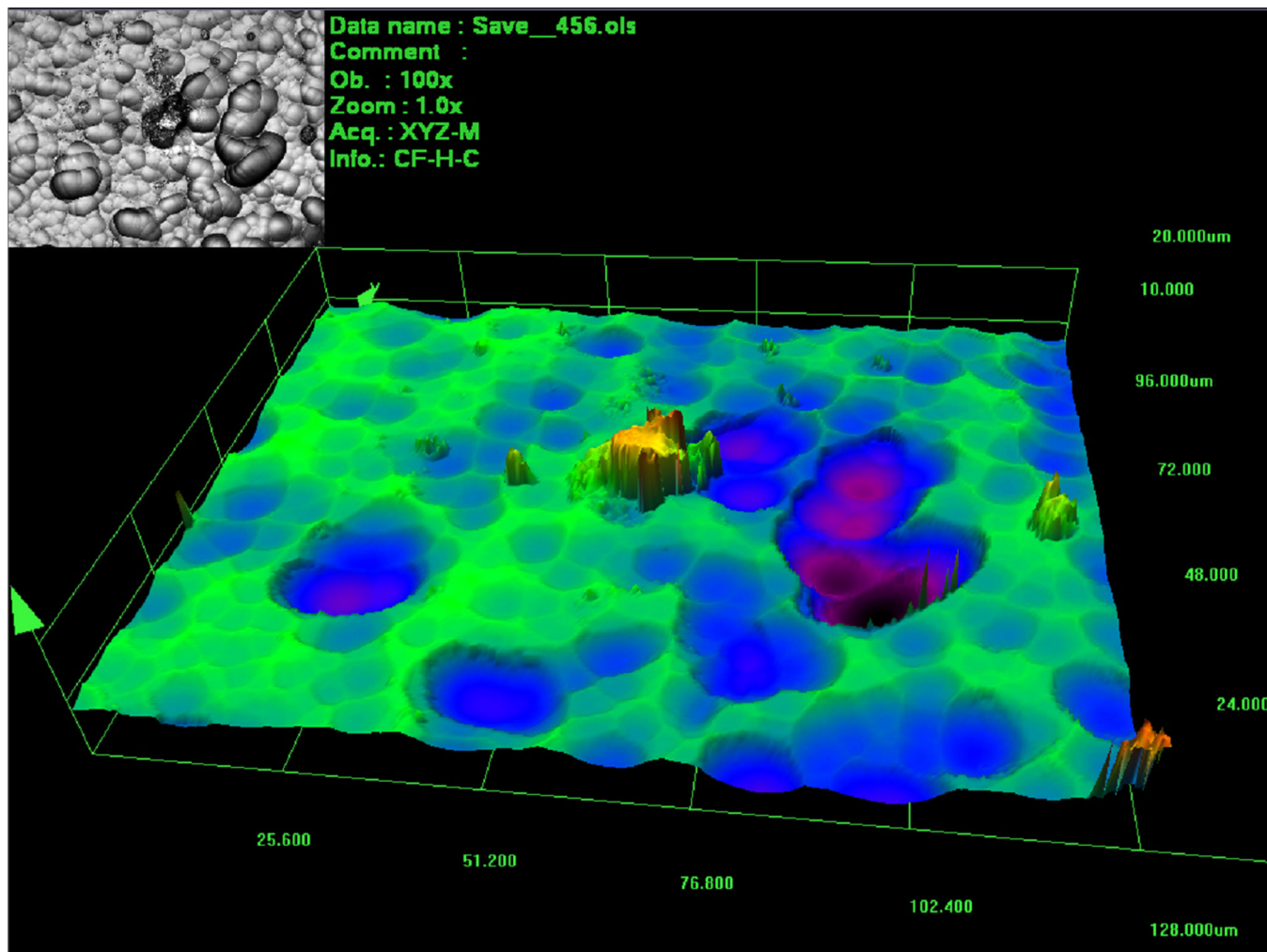


FIGURE 5 A micrograph of a silica glass plate after removing  $\sim 15 \mu\text{m}$  of the surface layer

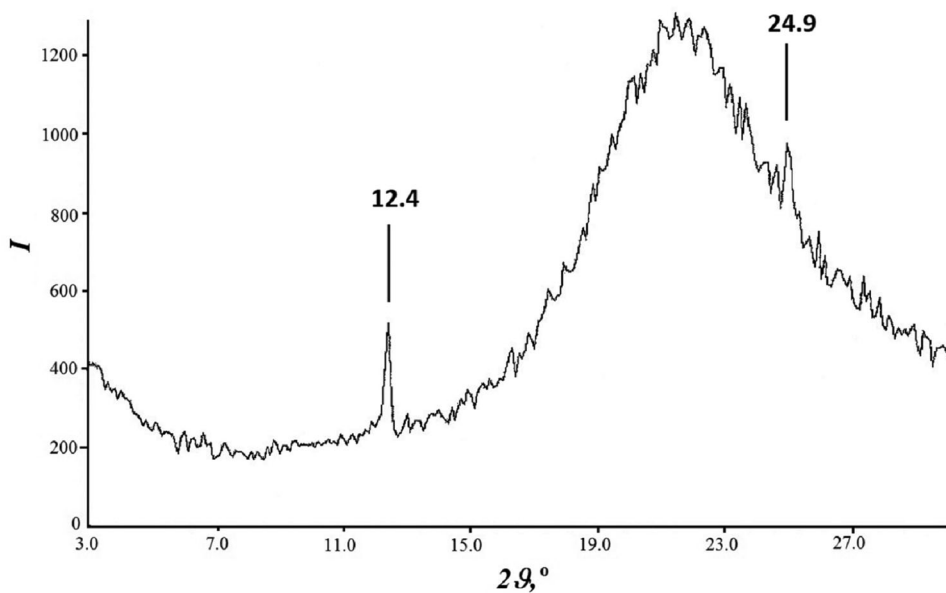


FIGURE 6 The diffractogram of the ground plate made from KU-1 glass

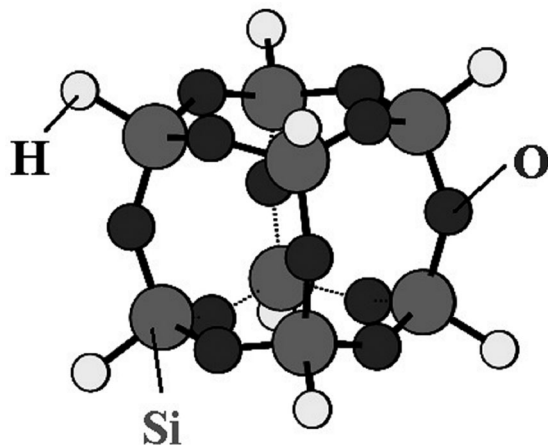


FIGURE 7 Schematic visualization of the  $H_8Si_8O_{12}$  cluster

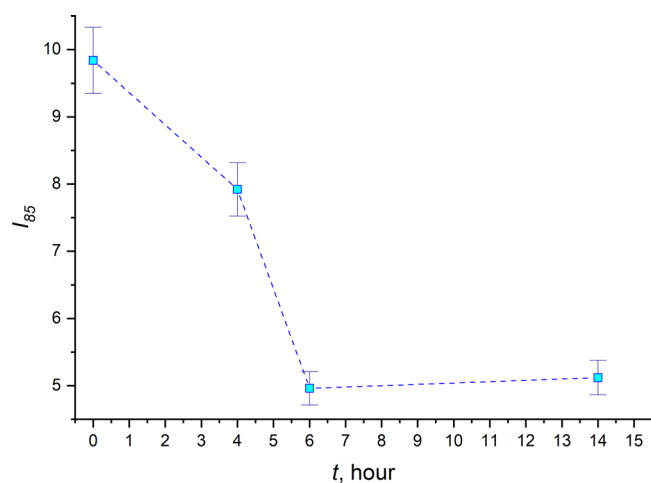


FIGURE 8 Height of the Raman  $I_{85}$  peak plotted against the annealing duration. Temperature of annealing:  $950^\circ\text{C}$

are being embedded into the atomic structure. An example of such a process, the hydroxylation of Si-O ring structures, is shown in Danchevskaya et al.<sup>25</sup>

### 3.2 | Breaking up of octahydrodoctasil-sesquioxane clusters during annealing

To verify our assumption about the formation of  $H_8Si_8O_{12}$  defects, a ground and deeply-etched silica plate was annealed at  $950^\circ\text{C}$ . The annealing temperature was chosen to be larger than the limit of temperature stability of  $H_8Si_8O_{12}$ , equal to  $\sim 850^\circ\text{C}$  according to Nicholson and Zhang.<sup>26</sup> The dependence of the  $I_{85}$  height against the annealing duration is shown in Figure 8. As was expected, the annealing leads to a decrease of the  $I_{85}$  peak and this can be linked with a reduction in the concentration of octahydrodoctasil-sesquioxane defects. However, the value of  $I_{85}$  did not decrease to zero but to a minimum level very

similar to the level of  $I_{85\text{min}}$  observed after the first stage of chemical etching (see Figure 4). Thus, some fractions of the  $H_8Si_8O_{12}$  clusters are not destroyed under the given annealing conditions.

This observation that some defects were formed close to the surface, while other defects were formed at the bottom of deep cracks, is worth discussion. Note that Nicholson and Zhang<sup>26</sup> described the breaking up of surface oxide layers formed after chemisorption of  $H_8Si_8O_{12}$  molecules on the surface of silicon crystals. The heating of the samples up to  $850^\circ\text{C}$  activates a process of evaporation of these layers from the surface. Heating up to  $700^\circ\text{C}$  leads to partial destruction of the oxide films, while some fraction of the clusters remains intact due to stabilization caused by reaction with the bulk of the substrate. We think this mechanism is relevant to the  $H_8Si_8O_{12}$  clusters observed in this study. However, clusters formed due to chemical modification of the bulk surface are more tightly bonded by intermolecular forces than chemisorbed layers. Clusters located at the bottom of deep cracks are even more embedded in the glass network since they are adhered to the bulk of the fused silica by a larger number of chemical bonds. Destruction and evaporation of such atomic clusters should require more energy. That is why the appearance of a small residual  $I_{85}$  peak after annealing at  $950^\circ\text{C}$  (in contrast to the effect observed in Nicholson and Zhang<sup>26</sup>) does not contradict our hypothesis. Perhaps crystalline octahydrodoctasil-sesquioxane defects can be destroyed at a higher temperature.

The annealed plate was chemically etched and cleaned again. The height of the  $I_{85}$  peak was immediately restored to its preannealing level. This indicates that the near-surface defects were formed again due to hydroxylation of the silica surface during chemical treatment in water.

### 3.3 | Rise of mechanical loss caused by octahydrodoctasil-sesquioxane defects

The hemispherical resonating shells used in navigation gyroscopes need to meet two requirements: The lowest mechanical loss and the greatest possible cylindrical symmetry.<sup>27</sup> The lowest mechanical loss (highest Q factor) was observed on polished, annealed, and carefully cleaned resonators. However, the polishing process modifies the shape of the resonators and interferes with their symmetry. Modern diamond tool lathes provide deviation from perfect symmetry of less than  $1\ \mu\text{m}$ , but the subsequent polishing by pressing with a lapping tool noticeably worsens the geometrical shape. This leads to vibration of the center of mass and additional losses at the point of resonator attachment.<sup>28,29</sup> This explains why the modern recommendation is to avoid polishing in the fabrication

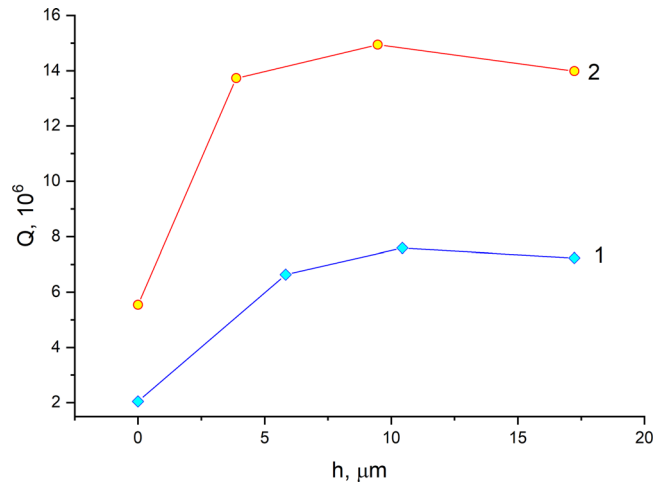


**FIGURE 9**  $Q$  factors of cylindrical fused silica samples plotted against depth of the removed surface layer. The samples were ground by an abrasive with grit particles of size: 1: 28  $\mu\text{m}$  and 2: 10  $\mu\text{m}$

process.<sup>30</sup> The surface of fused silica resonators processed with a diamond tool is close to a surface ground with a bonded abrasive tool. The  $Q$ -factor observed in such a resonator after chemical etching and cleaning may exceed  $10^7$ .<sup>31,32</sup> The precision correction of geometrical imperfection also can be done by controllable etching of the fused silica layers.<sup>33–35</sup> However, the crystalline  $\text{H}_8\text{Si}_8\text{O}_{12}$  defects that appear during etching presumably increase internal friction, and this effect deserves special attention.

We measured the  $Q$ -factor of cylindrical silica glass samples after chemical etching and cleaning and plotted it against the depth of the removed surface layer (Figure 9). The samples were ground by an abrasive with grit particles of size 10 and 28  $\mu\text{m}$ . As one might expect, the sample ground by the 10  $\mu\text{m}$  abrasive manifested a larger  $Q$ -factor. However, the  $Q$ -factor of both samples depends on the depth of the removed layer in the same way. Initially,  $Q$  increases rapidly as the damaged surface layer is removed. Further etching of the surface layer, when the removed thickness was more than 10  $\mu\text{m}$ , leads to reduction of the  $Q$ -factor. We believe this degradation may be caused by the growth of surface  $\text{H}_8\text{Si}_8\text{O}_{12}$  defects. The defects embedded in the surface of resonators act as structural heterogeneities which scatter mechanical energy, that is, increase dissipation or decrease  $Q$ -factor. Certainly, the contribution of such defects to the overall loss of mechanical energy merits further examination.

## 4 | CONCLUSION

Chemical etching of the ground surface of silica glass provokes the formation and further development of


microcrystalline defects deeply embedded in the atomic network of the near-surface layer. The chemical composition of these defects can be plausibly identified as  $\text{H}_8\text{Si}_8\text{O}_{12}$ . The formation of such defects is observed in both water-free silica glass-like KS4V and glass with high OH content like KU-1. The defects manifest themselves as a narrow peak near  $\nu \approx 85 \text{ cm}^{-1}$  in the Raman spectrum and as reflexes  $2\theta = 12.4^\circ$  and  $2\theta = 24.9^\circ$  on the diffractogram obtained by X-ray phase analysis. These defects were also detected by microscopic examination of the surface. The  $\text{H}_8\text{Si}_8\text{O}_{12}$  hypothesis has not only strengths but also some weaknesses. In particular, the relative height of the main Raman peaks observed in our experiments is different from the spectra reported in the literature. However, surface micro-crystalline defects were formed under very specific conditions; they are likely different in terms of size and the concentration of dislocations from crystalline samples reported before. That is why the  $\text{H}_8\text{Si}_8\text{O}_{12}$  hypothesis still merits consideration. The crystalline defects create structural heterogeneities in the near-surface layer of silica glass and increase dissipation. This phenomenon should be taken into account in the development of the technology of high- $Q$  silica resonator fabrication.

## ACKNOWLEDGMENTS

We are grateful to the Royal Society in the UK and the Russian Foundation for Basic Research which have allowed the authors to collaborate within the International Exchanges Scheme-2016 under Royal Society Cost Share Grant IE160125 and RFBR Grant 16-52-10069. We wish to thank all our colleagues from faculties of Physics and Chemistry at M.V. Lomonosov Moscow State University, the Institute for Gravitational Research at University of Glasgow, and the Aston Institute of Photonic Technologies at Aston University for help and support. We are also thankful to our colleagues from LIGO Scientific Collaboration and VIRGO Collaboration for their interest in our work. We would also like to show our gratitude to Dr. I. Martin and especially to Dr. V. Macaulay from University of Glasgow for proofreading of the paper draft. We would like to express sincere gratitude to our much-missed colleague, the late Dr. S.N. Torbin, who laid the foundations for this experimental study.

## ORCID

Boris S. Lunin  <https://orcid.org/0000-0001-8073-2559>

Kirill V. Tokmakov  <https://orcid.org/0000-0002-2808-6593>

## REFERENCES

- Ageev A, Palmer BC, De Felice A, Penn SD, Saulson PR. Very high quality factor measured in annealed fused silica.

- Class Quantum Gravity. 2004;21(16). <https://doi.org/10.1088/0264-9381/21/16/004>
2. Lunin BS, Tokmakov KV. Reduction in internal friction in silica glass with high OH content. *J Am Ceram Soc.* 2019;102(6):3329–40. <https://doi.org/10.1111/jace.16187>
  3. Ahamed MJ, Senkal D, Shkel AM. Effect of annealing on mechanical quality factor of fused quartz hemispherical resonator. In: 1st International Symposium on Inertial Sensors and Systems, Laguna Beach, CA, February 25–26, 2014. <https://doi.org/10.1109/ISISS.2014.6782512>
  4. Cho J, Yan J, Gregory JA, Eberhart H, Peterson RL, Najafi K. High-Q fused silica birdbath and hemispherical 3-D resonators made by blow torch molding. In: International Conference Micro Electro Mechanical Systems, Taipei, Taiwan, January 20–24, 2013. <https://doi.org/10.1109/MEMSYS.2013.6474206>
  5. Jeanroy A, Bouvet A, Remillieux G. HRG and marine applications. *Gyroscopy Navig.* 2014;5(2):67–74. <https://doi.org/10.1134/S2075108714020047>
  6. Aasi J., Abbott BP, Abbott R, Abbott T, Abernathy M, Ackley K, et al. Advanced LIGO. *Class Quantum Gravity.* 2015;32(7):074001. <https://doi.org/10.1088/0264-9381/32/7/074001>
  7. Aston SM, Barton MA, Bell AS, Beveridge N, Bland B, Brummitt AJ, et al. Update on quadruple suspension design for Advanced LIGO. *Class Quantum Gravity.* 2012;29(23):235004. <https://doi.org/10.1088/0264-9381/29/23/235004>
  8. Harry G, Billingsley G. Fused silica, optics and coatings. In: Reitze D, Saulson P, Grote H, editors. *Advanced interferometric gravitational-wave detectors.* Singapore: World Scientific Publishing Company; 2019. p. 521–54. [https://www.worldscientific.com/doi/abs/10.1142/9789813146082\\_0019](https://www.worldscientific.com/doi/abs/10.1142/9789813146082_0019)
  9. Devine RAB. *The physics and technology of amorphous SiO<sub>2</sub>.* New York, NY: Springer; 1988. <https://doi.org/10.1007/978-1-4613-1031-0>
  10. Wood RM, Thompson BJ. Selected papers on laser damage in optical materials. *SPIE Milestone Ser.* 1990;24:1–494.
  11. Skuja L. Optical properties of defects in silica. In: Pacchioni G, Skuja L, Griscom DL, editors. *Defects in SiO<sub>2</sub> and related dielectrics: science and technology.* Dordrecht: Springer; 2000. p. 73–116. [https://doi.org/10.1007/978-94-010-0944-7\\_3](https://doi.org/10.1007/978-94-010-0944-7_3)
  12. Bruckner R. Properties and structure of vitreous silica. I. *J Non Cryst Solids.* 1970;5(2):123–75. [https://doi.org/10.1016/0022-3093\(70\)90190-0](https://doi.org/10.1016/0022-3093(70)90190-0)
  13. TYDEX. Quartz glass for optics—the technical characteristics of the brands of fused silica KU-1 and KS4V. [cited 2021 May 5]. Available from: [http://www.tydexoptics.com/materials1/for\\_mirrors/fused\\_silica/](http://www.tydexoptics.com/materials1/for_mirrors/fused_silica/); [http://www.tydexoptics.com/pdf/Quartz\\_glass.pdf](http://www.tydexoptics.com/pdf/Quartz_glass.pdf)
  14. Popov SA, Nasyrov RS, Lebedev AS. Facility for making quartz glasses in vacuum and reactive-gas medium. *Glass Ceram.* 2012;68(9–10):306–7. <https://link.springer.com/article/10.1007/s10717-012-9376-6>
  15. Bouvestnik Innovation Center. The technical specifications of the diffractometers DRON for X-ray diffraction analysis. 2021 [cited 2021 May 5]. Available from: <https://bouvestnik.com/production/x-ray-diffraction-analysis/>
  16. ICDD. The powder diffraction file (PDF) [cited 2021 May 5]. Available from: <https://www.icdd.com/pdf-2/>
  17. Danchevskaya MN, Lunin BS, Torbin SN. Structure of surface defect layers of silica glass resonators. In: *Proceedings of the 17th International Congress on Glass.* Beijing: Chinese Ceramic Society; 1995. p. 137–41. Available from: [https://www.researchgate.net/publication/291975158\\_Structure\\_of\\_surface\\_defect\\_layer\\_of\\_silica\\_glass\\_resonators](https://www.researchgate.net/publication/291975158_Structure_of_surface_defect_layer_of_silica_glass_resonators)
  18. Suratwala T, Wong L, Miller P, Feit MD, Menapace J, Steele R, et al. Sub-surface mechanical damage distributions during grinding of fused silica. *J Non Cryst Solids.* 2006;352(52-54):5601–17. <https://doi.org/10.1016/j.jnoncrysol.2006.09.012>
  19. Miller PE, Suratwala TI, Wong LL, Feit MD, Menapace JA, Davis PJ, et al. The distribution of subsurface damage in fused silica. In: *Proceedings – Laser-Induced Damage in Optical Materials,* Boulder, CO; 2005. <https://doi.org/10.1117/12.638821>
  20. Marcolli C, Calzaferri G. Monosubstituted octasilasesquioxanes. *Appl Organomet Chem.* 1999;13(4):213–26. [https://doi.org/10.1002/\(sici\)1099-0739\(199904\)13:4<213::aid-aoc841>3.0.co;2-g](https://doi.org/10.1002/(sici)1099-0739(199904)13:4<213::aid-aoc841>3.0.co;2-g)
  21. Bärtsch M, Bornhauser P, Bürgy H, Calzaferri G. Infrared and Raman spectra of octa(hydridosilasesquioxanes). *Spectrochim Acta Part A Mol Spectrosc.* 1991;47(11):1627–29. [https://doi.org/10.1016/0584-8539\(91\)80258-K](https://doi.org/10.1016/0584-8539(91)80258-K)
  22. Bornhauser P, Calzaferri G. Ring-opening vibrations of spherosiloxanes. *J Phys Chem.* 1996;100(6):2035–44. <https://doi.org/10.1021/jp952198t>
  23. Raghavachari K, Eng J. New structural model for Si/SiO<sub>2</sub> interfaces derived from spherosiloxane clusters: implications for si 2p photoemission spectroscopy. *Phys Rev Lett.* 2000;85(5):935–8. <https://doi.org/10.1103/PhysRevLett.84.935>
  24. Handke B, Jastrzebski W, Kwaśny M, Klita L. Structural studies of octahydridoctasilasesquioxane—H<sub>8</sub>Si<sub>8</sub>O<sub>12</sub>. *J Mol Struct.* 2012;128:68–72. <https://doi.org/10.1016/j.molstruc.2012.06.033>
  25. Danchevskaya MN, Ivakin YD, Torbin SN, Muravieva GP. The role of water fluid in the formation of fine-crystalline oxide structure. *J Supercrit Fluids.* 2007;42:419–24. <https://doi.org/10.1016/j.supflu.2007.03.007>
  26. Nicholson K. T., Zhang K. Z., Banaszak Holl M. M., McFeely F. R. Reflection-absorption infrared investigation of hydrogenated silicon oxide generated by the thermal decomposition of H<sub>8</sub>Si<sub>8</sub>O<sub>12</sub> clusters. *J Appl Phys.* 2002;91(11):9043–48. <https://doi.org/10.1063/1.1469662>
  27. Armenise MN, Ciminelli C, Dell’Olio F, Passaro VMN. *Advances in gyroscope technologies.* Berlin, Heidelberg: Springer-Verlag; 2010. <https://doi.org/10.1007/978-3-642-15494-2>
  28. Izmailov EA, Kolesnik MM, Osipov A, Kolesnik A. Hemispherical resonator gyro technology. Problems and possible ways of their solutions. In: *Proceedings of the 6th International Conference on Integrated Navigation Systems,* St. Petersburg, Russia, May 24–26, 1999.
  29. Lunin BS. Problems and ways of development of hemispherical resonator gyroscope design. In: *Proceedings of the 12th International Conference on Integrated Navigation Systems,* St. Petersburg, Russia, 2005.
  30. Trusov AA, Phillips MR, Mccammon GH, Rozelle DM, Meyer AD. Continuously self-calibrating CVG system using hemispherical resonator gyroscopes. In: *International Symposium on Inertial Sensors and Systems.* March 23–26, 2015. <https://doi.org/10.1109/ISISS.2015.7102362>



31. Lunin BS, Matveev VA, Basarab MA. The wave wave solid-state gyroscope. Theory and technology. Moscow: Radiotekhnika; 2014.
32. Lunin BS, Torbin SN. Internal friction in quartz glass at moderate temperatures. Moscow Univ Chem Bull. 2000;55(2)30–2.
33. Wang Y, Pan Y, Qu T, Jia Y, Yang K, Luo H. Decreasing frequency splits of hemispherical resonators by chemical etching. Sensors. 2018;18(11):3772. <https://doi.org/10.3390/s18113772>
34. Basarab MA, Lunin BS, Matveev VA, Chumankin EA. Balancing of hemispherical resonator gyros by chemical etching. Gyroscopy Navig. 2015;6(3):218–23. <https://doi.org/10.1134/S2075108715030025>
35. Tao Y, Pan Y, Jia Y, Liu J, Tan Z, Yang K, et al. Frequency tuning of fused silica cylindrical resonators by chemical etching. 2019 DGON Inertial Sensors and Systems (ISS), Braunschweig, Germany. 2019:1–20. <https://doi.org/10.1109/ISS46986.2019.8943661>

**How to cite this article:** Lunin BS, Tokmakov KV. The formation of microcrystalline defects on the surface of silica glass arising from mechanochemical processing. *Int J Appl Glass Sci.* 2022;13:655–663. <https://doi.org/10.1111/ijag.16558>